JOURNAL OF Materials CHEMISTRY

Sol–gel synthesis of monolithic tin-doped silica glass†

N. Chiodini, F. Morazzoni, A. Paleari, R. Scotti* and G. Spinolo

INFM—Dipartimento di Scienza dei Materiali, Università di Milano-Bicocca, via Cozzi 53, 20125 Milano, Italy. E-mail: Roberto.Scotti@mater.unimib.it

Received 2nd June 1999, Accepted 3rd August 1999

The preparation of Sn-doped SiO_2 glasses with different Sn contents ($Sn/(SiO_2+SnO_2)$ ratio 0.01 to 10.0% w/w) was performed by two sol–gel routes. The first route (method A) used tin(IV) *tert*-butoxide as the tin precursor and in the presence of acetylacetone it resulted in transparent glasses with a maximum tin content of 0.1%. The precursor in the second route (method B) was dibutyltin diacetate; this was more efficient and transparent glasses of up to 1% tin content were obtained. As electron paramagnetic resonance can identify paramagnetic E′ Sn centres, defects that form when silica glass is subjected to X-ray irradiation, we assessed the tin centres that substituted silicon in the silica network.

At higher tin contents ($Sn \geqslant 3\%$), method B gave crystalline nanosized particles of SnO_2 (6–10 nm) dispersed throughout the silica matrix.

Introduction

Since 1978, when Hill *et al.*[1] discovered that a permanent refractive index grating could be produced by the interference of visible waves within a Ge-doped silica fiber core, silica materials have been extensively studied in an effort to understand the mechanisms involved in light-induced refractive index changes and microscopic structural modifications in the oxide.[2] Different models have been proposed to explain the origin of photorefractivity, *e.g.* the colour-centre model[3,4] and the densification model.[5] Although neither the physics nor the chemistry of the process have yet been fully understood, photorefractive properties are generally associated with the presence of Ge related defect centres.[6] In fact it has been recognised that the E′ Ge centres, three-coordinated Ge sites with an unpaired electron in a sp^3 orbital, are connected with increased refractive index values.[7]

Research has also been directed towards the enhancement of the sensitivity and long-term stability of gratings in silica fibers. In order to obtain these effects, many authors attempted to dope silica with elements other than Ge (*e.g.* aluminium, phosphorus, rare-earth metals). These materials were generally found to have a photosensitivity comparable with Ge-doped silica or even somewhat less.[2] Interestingly Sn-codoped germanosilicate fibers show a larger photoinduced refractive index change and a significant improvement of the grating thermal stability without any loss of optical properties.[2,8] Thus the development of a suitable method to dope silica glass with tin could facilitate studies into photoactivated processes.

The sol–gel technique, *via* the hydrolysis and condensation of molecular precursors at low temperatures, has been used[9] to prepare doped silica materials, instead of high temperature methods.[10] The sol–gel method allows easier control of the composition; furthermore preforms for fibers and films for planar waveguides can be produced. However when precursors of different elements undergo hydrolysis, different gelation rates could lead to a lack of homogeneity in the gels.

Silica gel is usually prepared by the hydrolysis and condensation of a silicon alkoxide in alcohol solution.[11] On the other hand the gelation of metal alkoxides like Sn is difficult to control as they are highly reactive with water and upon hydrolysis precipitate as hydroxo or oxohydroxo compounds. This is because metals are less electronegative than silicon and have a tendency to increase their number of coordination ligands, substituting the alkoxy groups with water.[12,13] The more electropositive and the less coordinated the metal, the easier the hydrolysis.

Different approaches have been followed to obtain multi-component homogeneous gels from alkoxides: the hydrolysis of heterometal alkoxides containing two, three or four different metal atoms in the same precursor molecule;[14] the sequential addition of the alkoxides of different elements, in ascending order of reactivity to the partially hydrolysed alkoxide of lower reactivity;[15] a non-hydrolytic route based on condensation between metal chlorides and either alkoxides or ethers.[16]

The present paper describes two new sol–gel routes for the preparation of Sn-doped SiO_2 xerogels and the sintering process of xerogels to obtain monolithic glasses. The goal of both preparation methods was to produce a homogeneous gel from a sol phase where the silicon precursor tetraethoxysilane (TEOS) and a non-chlorinated tin precursor were mixed, avoiding the sudden precipitation of tin hydroxides or oxohydroxides.

In the first method (A) the goal was reached by adding a chelating ligand, acetylacetone (acacH), to the sol phase to retard the hydrolysis and condensation of the tin precursor, tin(IV) *tert*-butoxide (TTBO), which actually has a higher reactivity toward water than TEOS. TTBO was chosen as the tin precursor because it is monomeric in both the solid state and in solution, unlike tin isopropoxide, which has a dimeric structure.[17] acacH transfers its acidic proton to an alkoxide ligand, which yields the corresponding alcohol, and the acetylacetonate anion (acac) coordinates to the precursor. The modified tin precursor has a lower reactivity as acac is more resistant to hydrolysis than alkoxide.[18,19]

In the second method (B) a less reactive tin precursor, dibutyltin diacetate (DBTDA), was mixed with TEOS in the sol phase. In fact carboxylates hydrolyse more slowly than alkoxides;[20] the two alkyl groups cannot be substituted by water, as reported for di- and tri-alkyltin compounds.[21]

Sn-doped SiO_2 glasses of different Sn contents (percentage of Sn ranged from 0.01 to 10.0% w/w) were prepared by both methods. The aim was to obtain transparent monolithic xerogels and glasses where tin atoms replaced silicon centres in the silica network. The presence of paramagnetic E′ Sn centres, which can be easily formed by X-ray irradiation of Sn-doped silica and identified by electron paramagnetic resonance

†Electronic supplementary information (ESI) available: colour version of Fig. 2. See http://www.rsc.org/suppdata/jm/1999/2653/

(EPR) spectroscopy,[22] verified that the Sn atoms were located in the silica structure in the silicon atoms position and revealed the degree to which the substitutional Sn atom number depended on the dopant amount and preparation method.

X-Ray diffraction (XRD) was used to identify crystalline phases after sintering and to roughly estimate their mean grain size. Raman spectra indicated the structural modification of the silica glass in the presence of Sn dopant, and assessed the formation of nanosized SnO_2 particles. The optical absorption properties of the glasses were studied in the UV-visible region.

Experimental

Synthesis methods

Tin doped silica xerogels with increasing Sn contents (Sn/(SiO_2+SnO_2) ratio: 0.01, 0.05, 0.1, 0.5, 1.0, 3.0, 5.0, 10.0% w/w) were prepared by two different methods, A and B. The flow-chart in Fig. 1 sums up the steps of the experimental procedures.

Method A. Reagents: tin(IV) *tert*-butoxide (TTBO), synthesised by slight modification of the method proposed by Hampden-Smith *et al.*,[23] sublimated twice; tetraethoxysilane (TEOS), Strem Chemicals 99.9999%; acetylacetone (acacH), Fluka HPLC grade reagent; ethanol, HPLC grade reagent; water, mQ.

A solution of TTBO was first prepared by dissolving, under nitrogen, 1.88 g (4.57 mmol) of TTBO in a solution of 7.00 ml (120 mmol) of ethanol and 3.00 ml (29.1 mmol) of acacH.

The solutions of the different samples were prepared in polypropylene containers, adding in succession and under stirring 3.00 ml (29.1 mmol) of acacH, 2.50 ml (11.2 mmol) of TEOS, an amount of TTBO solution which varied with the tin amount (*e.g.* for the 10% sample 1.41 ml of TTBO solution, equivalent to 0.644 mmol of TTBO) and a solution of 4.00 ml (68.6 mmol) of ethanol and 1.50 ml (83.3 mmol) of water.

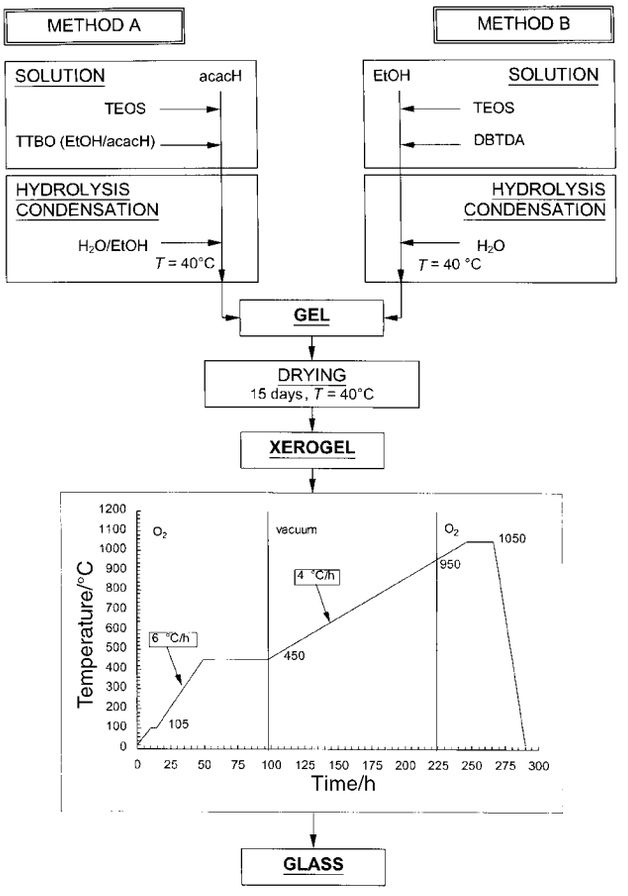

Fig. 1 Flow-chart of the experimental procedures (TEOS = tetraethoxysilane; TTBO = tin(IV) *tert*-butoxide; acacH = acetylacetone; DBTDA = dibutyltin diacetate; EtOH = ethanol).

The molar ratio Si : H_2O : EtOH : acacH (1 : 7.4 : 7.6 : 3.0) was the same for the whole tin content range. AcacH was in large excess with respect to tin (*e.g.* for the 10% sample the molar ratio acacH : Sn was about 50).

The containers were sealed with a polyethylene film and put into a thermostatic chamber at 40 ± 1 °C. Three small holes in the film (about 1 mm diameter) allowed the solvents to evaporate.

Gelation times were recorded when the sol phase lost its liquid characteristics and was transformed into a continuous phase, incorporating the total amount of solvent and holding the shape of the container.

Gelation times for different tin precursor contents are reported in Table 1. The absolute values have an uncertainty of about ±30% but the relative trend *vs.* tin content was confirmed by repeated experiments.

After gelation the samples were dried in a thermostatic chamber at 40 ± 1 °C for 15 days.

The glasses were obtained from the xerogels by the sintering process shown in Fig. 1: the samples were heated (heating rate 10 °C h^{-1}) under an oxygen stream up to 105 °C and maintained at this temperature for 4 h; heated (10 °C h^{-1}) under an oxygen stream up to 450 °C and maintained at this temperature for 48 h; heated (4 °C h^{-1}) in vacuum (1.33 Pa) up to 950 °C; heated under an oxygen stream up to 1050 °C (4 °C h^{-1}) and finally maintained at this temperature for 20 h.

Plates of about 15 mm diameter and 2 mm thick were obtained (Fig. 2).

Thermogravimetry (TGA) measurements performed on xerogels from 20 to 1050 °C in air showed that there was a mass loss of about 18% between room temperature and 125 °C. This loss was attributed to the evaporation of organic reagents and physisorbed water. A further 5% mass loss occurred between 125 and 535 °C and can be attributed to different binding sites within the silica network with different bond strengths. A minor mass loss, about 2%, also occurred at higher temperature, between 535 and 1050 °C, and this was also probably due to hydroxyl groups.

BET surface area measurements were performed on xerogels during the thermal treatment, stopping the sintering process at intermediate temperatures; there was a marked decrease in surface area with increasing treatment temperature. Example: sample 0.05%, surface area of xerogel before thermal treatment, 605 m^2 g^{-1}, xerogel sintered at 550 °C, 472 m^2 g^{-1}; at 750 °C the surface area was lower than the detection limit of the instrument (< 1 m^2 g^{-1}).

Tin analysis performed by inductively coupled plasma-atomic emission spectroscopy (ICP-AES) revealed no loss of tin during thermal treatment.

Method B. Reagents: dibutyltin diacetate (DBTDA), Fluka; tetraethoxysilane (TEOS), Strem Chemicals 99.9999%; ethanol, HPLC grade reagent; water mQ.

The solutions were prepared in polypropylene containers by adding successively, under stirring, 7.00 ml (120 mmol) of ethanol, 2.50 ml (11.2 mmol) of TEOS, the appropriate amount of DBTDA and 1.50 ml (83.3 mmol) of water. In the 10% sample, DBTDA was added pure (0.175 ml equivalent to 0.649 mmol). In samples with lower tin contents, DBTDA was added in ethanol solution (1 ml DBTDA: 10 ml ethanol for 0.5–5% samples; 1 ml: 50 ml for 0.01–0.1% samples).

The molar ratio Si : H_2O : EtOH (1 : 7.4 : 10.7) was the same for the whole range of tin contents.

The containers were sealed with a polyethylene film and put into a thermostatic chamber at 40 ± 1 °C. Three small holes in

Table 1 Preparation of gels and glasses

Sample		Method A			Method B		
$Sn/(SnO_2+SiO_2)$[a] %w/w	Sn/Si mol/mol	Gelation time/h	Xerogel	Glass	Gelation time/h	Xerogel	Glass
0	—	48			72		
0.01	5.8×10^{-5}	48		Transparent	72		Transparent
0.05	2.9×10^{-4}	96	Transparent	Colourless	66		Colourless
0.1	5.8×10^{-4}	144	Colourless		60		
0.5	2.9×10^{-3}	192		Yellow	48	Transparent	
1	5.8×10^{-3}	200			36	Colourless	
3	1.7×10^{-2}	1.5	Opaque	Opaque	24		Yellow
5	2.9×10^{-2}	0.75	White	White/yellow	24		
10	5.8×10^{-2}	0.25			24		

[a]Starting mixture composition.

the film (about 1 mm diameter) allowed the solvents to evaporate.

Gelation times for different tin precursor contents are reported in Table 1. The absolute values have an uncertainty of about $\pm30\%$ but the relative trend *vs.* tin content was confirmed by repeated experiments.

After gelation, drying to xerogels and the sintering process to glass were performed as in method A.

TGA measurements performed on xerogels from 20 to 1050 °C in air showed mass losses similar to those exhibited by samples prepared *via* method A.

The BET surface area decreased markedly with increasing treatment temperature. Example: sample 0.01%, surface area of xerogel before thermal treatment, 687 $m^2\ g^{-1}$, xerogel sintered at 673 K, 571 $m^2\ g^{-1}$; at 750 °C the surface area was lower than the detection limit of the instrument ($<1\ m^2\ g^{-1}$).

Tin analysis performed by ICP-AES revealed that no loss of tin occurred during the thermal treatment.

Analytical procedures and spectroscopic measurements

The BET surface area measurements were performed on a Coulter SA 3100 instrument after outgassing the samples at 100 °C for 60 min.

TGA measurements were performed on xerogels from 20 to 1050 °C in air with a heating rate of 5 °C min^{-1}.

ICP-AES analysis of tin was performed with a Jobin-Yvon 38 instrument. The glass (about 60 mg) was first dissolved in a 48% w/w solution of HF (about 10 ml). After addition of conc. H_2SO_4 (0.5 ml), the solution was heated to eliminate fluorides, then diluted with H_2O in a volumetric flask (10 ml) and the tin content measured.

Optical absorption spectra were recorded between 190 and 700 nm by using a Cary 2300 Varian spectrophotometer operating under flowing nitrogen.

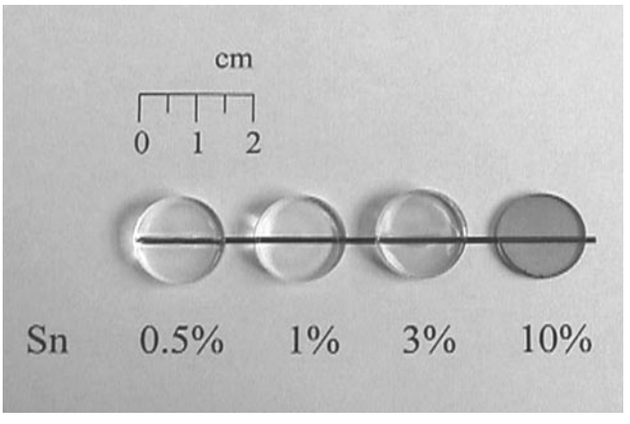

Fig. 2 Monolithic glass of tin doped silica produced by method B. The tin content is indicated. (For a full-colour version of this figure, see http://www.rsc.org/suppdata/jm/1999/2653/)

Raman measurements were performed by using a Labram Dilor microRaman spectrometer excited by a He–Ne laser in back-scattering configuration. Relative peak positions were determined with a final precision of about 1 cm^{-1}. Relative peak intensities were analysed by normalising the spectra at the intrinsic ω_3 mode of SiO_2 at 800 cm^{-1}, which is well separated from all other peaks. Differential spectra showing the isolated pattern of the SnO_2 nanophase (see Results) were normalised to the main peak at 638 cm^{-1} attributed to the A_{1g} mode of crystalline SnO_2.

EPR spectra were recorded at 25 °C by using a Bruker EMX spectrometer operating at the X band and magnetic field modulation of 100 kHz, with a microwave power of 1 mW and a modulation amplitude of 0.3 G. The microwave frequency was accurately read with a HP 53131A frequency counter and the g values were calculated by comparison with a l standard ($g=2.0036$). The amount of paramagnetic species was calculated by double integration of the resonance line area. Before EPR measurements the samples were irradiated at 25 °C by means of an X-ray tube (W target, 32 kV, 20 mA) at a dose of about 2×10^4 Gy.

The powder XRD patterns were obtained under ambient conditions with a Siemens D500 diffractometer using monochromatic Cu-Kα radiation ($\lambda=1.5418$ Å). The average crystallite size D of SnO_2 particles dispersed in silica glass was calculated by the reflection from the (110) plane according to the Scherrer formula, $D=0.9\lambda/(\beta\cos\theta)$, where λ is the wavelength of the X-rays, 2θ is the diffraction angle. $\sqrt{\beta_n^2-\beta_s^2}$ is the corrected halfwidth in radians, with β_n the observed (110) reflection halfwidth of SnO_2 in Sn-doped silica samples and β_s the halfwidth in a standard sample of SnO_2 powder. The standard sample of SnO_2 was obtained by sintering a powdered xerogel of pure SnO_2 prepared by method B at 1050 °C in oxygen for 24 h.

Results

Synthesis

The gelation time and the physical properties of the xerogels and glass depended on both the preparation method and the amount of tin (Table 1). By using method A, the gelation time increased with low tin contents (0–0.5%); transparent and homogeneous xerogels were obtained by drying the samples at 40 °C after gelation. At higher dopant contents (3–10%) the gelation times decreased dramatically, the sol–gel transition being much faster than for low contents (*e.g.* 0.5%, 192 h; 3%, 1.5 h); opaque and inhomogeneous xerogels were obtained. A 1% sample showed a different behaviour, producing an opaque xerogel after a very long gelation time.

With method B, the gelation time for the whole composition range (0–10%) gradually decreased with increasing tin content ranging from 72 to 24 h; transparent and homogeneous xerogels were formed.

After the sintering process, the xerogels produced by method B gave rise to transparent monolithic glasses. They were colourless at less than 1% Sn content but for larger amounts of dopant (3, 5 and 10%) they became yellow (Table 1, Fig. 2; see colour version of Fig. 2 deposited as ESI [see first page of article]).

Transparent colourless glasses was also obtained when the xerogels were sintered by method A, provided that the tin content was less than 0.5% (Table 1). At 0.5% the glass was slightly yellow and at higher dopant contents the samples broke up during the sintering process and appeared opaque, white-yellow and inhomogeneous.

An optical absorption spectrum of the yellow glass showed an absorption edge at 340 nm, with a tail at wavelengths higher than 400 nm, which was the origin of the visible colour. The colourless glass showed no absorption band above 200 nm. The edge at 340 nm corresponded to the energy gap of SnO_2, 3.6 eV.[24]

This behaviour was due to the presence of nanosized particles of SnO_2, as revealed by XRD analysis. The diffraction patterns of the yellow glass produced by method B (Sn contents 3, 5 and 10%) showed the cassiterite crystalline structure (Fig. 3).[25] The peak intensities increased with the tin content. The average size of the SnO_2 grains dispersed in the silica was calculated using the Scherrer formula, and was found to range from 6 nm (3%) to 10 nm (10%).

No crystalline phase was evident at lower tin contents.

Traces of nanosized particles of SnO_2 also occurred in the 0.5% yellow glass produced *via* method A. The inhomogeneous samples obtained using this method for higher tin contents precluded the detection of significant diffraction patterns. In any case the presence of a phase of SnO_2 was clearly supported.

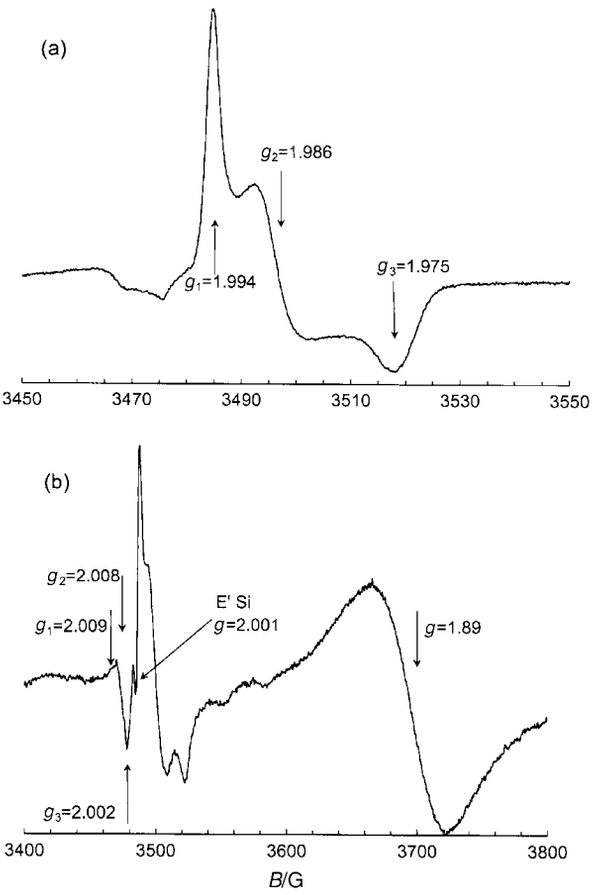

Fig. 4 (a) EPR spectrum at 298 K of E′ Sn defects in Sn-doped silica glass (Sn 0.5% w/w, method B); (b) EPR spectrum at 298 K of Sn-doped silica glass (Sn 10% w/w, method B).

EPR spectra

EPR spectra of X-ray irradiated glasses prepared by both methods A and B showed the signals of the E′ Sn centres in an orthorhombic symmetry field with $g_1 = 1.994$, $g_2 = 1.986$, $g_3 = 1.975$ whatever the amount of dopant the glass contained (as an example the EPR spectrum of the 0.5% sample produced *via* method B is reported in Fig. 4a). The assignment of E′ Sn centres was supported by comparison with the resonance lines previously observed in Sn-doped SiO_2 after X-ray irradiation.[22]

The spectra of all the samples also showed the signals of silicon-related defects in irradiated silica. These were the narrow asymmetric line at about $g = 2.001$ attributed to E′ Si centres[22,26] and the resonances attributed to oxygen related sites, non-bridging oxygen hole centres ≡Si–O• and peroxy radicals ≡Si–O–O•, at g values of 2.002, 2.008 and 2.009.[27]

The EPR intensities of E′ Sn centres increased with the amount of dopant in the colourless glass, but were significantly lower in both the opaque inhomogeneous and the yellow glass where the presence of SnO_2 particles was observed (Fig. 5).

Furthermore, in the yellow glass a symmetric resonance line was observed at $g = 1.890$ (Fig. 4b). This signal is identical to that of the singly ionised oxygen vacancies in SnO_2, already observed in pure SnO_2 powder after thermal treatment under vacuum[28] or under reducing gases.[29]

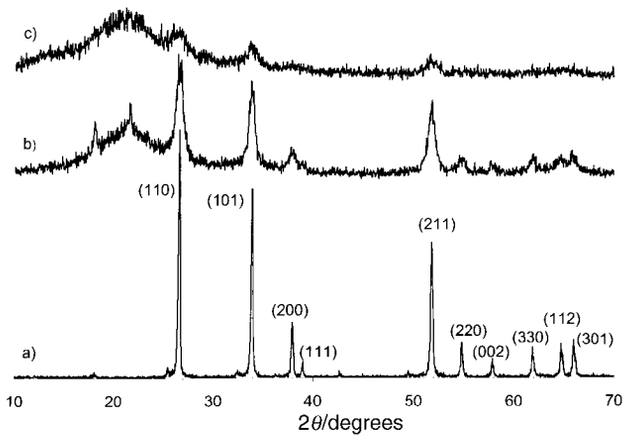

Fig. 3 XRD patterns of (a) SnO_2 powder reference (*hkl* Miller indices are indicated); (b) Sn-doped silica glass prepared by method B (Sn 10% w/w); (c) Sn-doped silica glass prepared by method B (Sn 3% w/w).

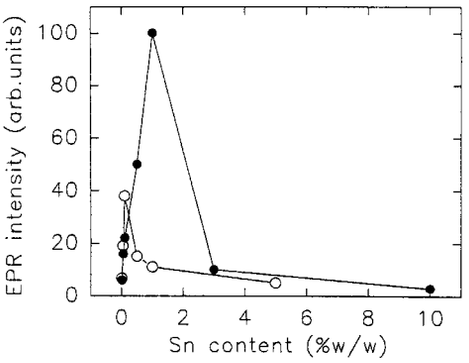

Fig. 5 EPR intensities of E′ Sn signals *vs.* Sn content, expressed as Sn % w/w, for X-ray irradiated glasses prepared by method A (○) and method B (●).

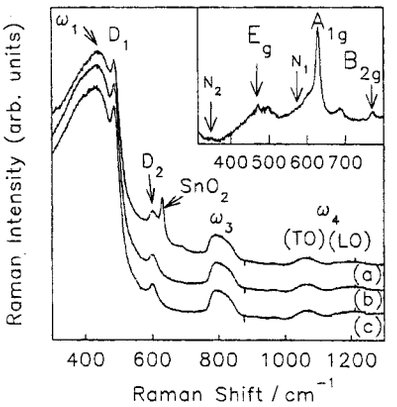

Fig. 6 Raman spectra of SiO_2 samples obtained by method B with (a) 10%, (b) 0.5% and (c) 0% of Sn. In the inset the difference between spectra (a) and (c) is reported, showing the Raman features of the SnO_2 nanophases.

Raman spectra

The Raman spectra (300–1300 cm^{-1}) of Sn-doped silica glasses were typical of pure silica glass up to a Sn content of 0.5% for method A and 1% for method B, and no peak attributable to vibrational modes directly involving Sn atoms was observed. As an example, Fig. 6 shows the Raman spectrum of a 0.5% sample (method B) compared with that of pure silica. The main bands of the silica spectrum are indicated: the D_1 and D_2 peaks at 490 and 610 cm^{-1}, attributed to symmetric stretching modes of vibrationally isolated four-fold and three-fold rings of SiO_2 tetrahedra;[30–32] the band at 440 cm^{-1}, attributed to the symmetric stretching ω_1 mode of SiO_2;[33,34] the bands at 800 cm^{-1} (ω_3 mode), 1060 cm^{-1} (transverse optic (TO) ω_4 mode) and 1190 cm^{-1} (longitudinal optic (LO) ω_4 mode).[33]

The results showed that the Sn-doping induced a slight shift of the ω_1 and ω_4 (TO) modes of the SiO_2 Raman spectrum upon increasing the Sn content to 0.5% with method A and 1% with method B (Fig. 7). This effect is related to a decrease of the mean Si–O–Si angle, accompanied by a weakening of the Si–O bonds.[35,36]

The effect stopped when the Sn content increased above 0.5% (method A) and 1% (method B) and a peak appeared at about 630 cm^{-1} corresponding to the A_{1g} mode of crystalline SnO_2[36] (Fig. 6). The intensity of the SnO_2 A_{1g} mode increased with increasing Sn content (Fig. 7). The difference between the spectra of the 10% sample and pure silica (inset in Fig. 6) highlights two other Raman active modes of crystalline SnO_2, E_g at 476 cm^{-1} and B_{2g} at 782 cm^{-1}.[37]

The intensity ratio between the volume and surface modes of the Raman spectra gives some indication of the SnO_2 grain

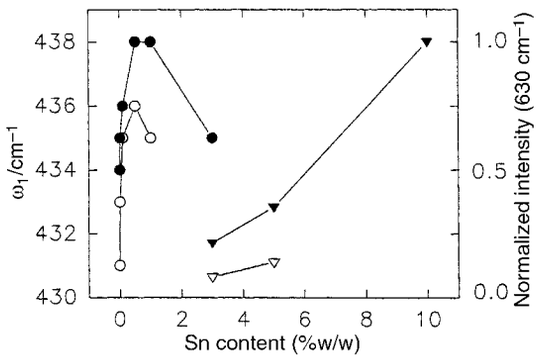

Fig. 7 Sn-doping effects on the Raman spectra of the investigated samples: shift of the SiO_2 ω_1 mode at low Sn content (circles) and growth of the A_{2g} mode of SnO_2 at heavy doping (triangles), in samples produced from method A (open symbols) and method B (filled symbols).

dimensions. In samples where the SnO_2 phase was detected, the intensity of the A_{1g} Raman allowed mode of crystalline SnO_2 can be compared with the intensity of a surface-related N_2 mode at about 350 cm^{-1}.[25,38–40] This mode was unobservable in SnO_2 unless the size d of the crystallites fell below 13 nm.[38,39] Typical nanosized SnO_2 particles with $d<5$ nm should show a broad band N_1 at about 580 cm^{-1}, with an intensity comparable with that of the 630 cm^{-1} peak. This band was not observed in our differential spectra, probably being hidden in the background due to the imperfect subtraction of the SiO_2 Raman features. This indicated that its intensity was definitely lower than that of the 630 cm^{-1} peak, and that the dimensions of the SnO_2 nanophases formed in our samples were larger than 5 nm but smaller than 13 nm, in agreement with the XRD results.

Discussion

Both the proposed preparation methods A and B were suitable for obtaining colourless transparent monolithic glasses of Sn-doped silica in a range of tin contents which depended on the method used.

In both methods the silica gelation process was affected by the presence of tin, as deduced from the variation in gelation times with increasing tin content (Table 1). The gelation rates were determined by the amount of tin and differed for the two methods A and B.

In method B the acetate ligands of the DBTDA precursor probably undergo slower hydrolysis than the alkoxide ligands, allowing the simultaneous gelation of the tin and silicon precursors. The gelation times gradually decreased upon increasing the amount of precursors and the xerogels were homogeneous throughout the whole range of composition investigated.

With procedure A the added acacH could act as a chelating agent and the ligand acac was more resistant to hydrolysis than the alkoxide; in fact at low tin contents the presence of acac retarded the hydrolysis and condensation of the precursors. Transparent colourless glasses were obtained with a maximum amount of tin of 0.1%, ten times less than by method B. At higher tin contents ($\geqslant$1%) the chelating effect is less efficient, though the ratio acacH : (Si,Sn) was about 3 : 1. The molecules of the tin precursors underwent fast condensation to give an inhomogeneous gel phase.

In the colourless transparent glasses Sn atoms were located substitutionally in the silica network, regardless of the preparation method used, as indicated by the formation of E′ Sn centres under X-ray irradiation. In fact E′ Sn centres, initially recognised by our group,[22] consist of a three-coordinated Sn with an unpaired electron in an sp^3 orbital and have the same electronic configuration as isoelectronic Ge and Si E′ centres. The amount of E′ Sn increased with increasing tin content and dramatically decreased in all samples (opaque and yellow) where the SnO_2 crystalline phase formed (Fig. 5).

E′ Sn centres could have both axial and rhombic symmetry,[29] depending on the presence of non-equivalent oxygen atoms in the tin coordination field. E′ Sn centres in the glasses reported here had only rhombic symmetry; this may be attributable either to oxygen atoms bridging two Sn centres or to the formation of peroxy linkages with the oxygen atoms bonded to the E′ Sn centres.

The fact that there is a slight probability of two tin atoms being bridged by oxygen (about 17 Si atoms per Sn atom in 10% and 17000 in 0.01% samples) suggests that distortion is not caused by a neighbouring Sn atom even if it can not be completely excluded that Sn–O–Sn bonds could be favoured compared to Sn–O–Si, the hydrolysis–condensation kinetics of tin being different from that of silicon. According to Griscom's

model[26] for the E'_{α} centres, a rhombic variant of E′ Si, it can be suggested that radiolytic breaking of an Sn–O bond causes both the formation of an E′ Sn centre and the displacement of the oxygen atom from its normal position. This oxygen atom forms a peroxy linkage with a near-neighbour oxygen of an E′ Sn centre and the new O–O bond is the reason for the rhombic distortion.

The Raman results also confirmed that tin atoms substituted for silicon in the silica network. In spite of the absence of vibrational modes directly involving Sn atoms, the shift of the intrinsic modes ω_1 and ω_4 (TO) with different amounts of dopant showed that tin atoms induced local stresses in the silica network, thus modifying the mean Si–O–Si linkage geometry.

According to the above-mentioned conclusions, segregation of a SnO_2 phase led to a decrease of the Sn-doping effect on the shift of the ω_1 and ω_4 (TO) modes (Fig. 7) and, furthermore, the number of E′ Sn centres decreased (Fig. 5).

Homogeneous yellow glasses were obtained by sintering transparent xerogels with higher tin contents. This yellow colour mainly occurred in glasses prepared by method B ($Sn \geqslant 3\%$), although a method A sample with 0.5% tin content showed similar characteristics. This glass contained a crystalline SnO_2 phase with particle dimensions ranging between 6 and 10 nm. The nanosized particles were well dispersed throughout the silica matrix, deduced from the lack of light scattering in the visible region. The tail of the absorption edge at 340 nm, due to SnO_2, explained the yellow colour of the glass.

Conclusions

Two synthetic sol–gel routes for the preparation of monolithic Sn-doped silica glass were studied. Method A used tin(IV) *tert*-butoxide as the tin precursor in the presence of acetylacetone and produced transparent monolithic glasses with a maximum tin content of 0.1%. Method B used dibutyltin diacetate as the precursor. It was more efficient and led to transparent glasses with a higher tin content, up to 1%.

The substitutional character of the Sn atoms in the silica network was assessed by the presence of paramagnetic E′ Sn centres, easily formed by X-ray irradiation, which were characterised by EPR spectroscopy.

In the glass prepared by method B with $Sn \geqslant 3\%$ a crystalline nanophase of SnO_2 (main dimensions 6–10 nm) well dispersed throughout the silica matrix was identified.

Acknowledgements

This research was supported by a national project of MURST and the authors wish to thank N. Morgante for XRD measurements and A. Lazzarini for technical support.

References

1 K. O. Hill, Y. Fujii, D. C. Johnson and B. S. Kawasaky, *Appl. Phys. Lett.*, 1978, **32**, 647.
2 B. Poumellec and F. Kherbouche, *J. Phys. III*, 1996, **6**, 1595.
3 D. P. Hand and P. S. J. Russel, *Opt. Lett.*, 1990, **15**, 102.
4 R. M. Atkins, V. Mizrahi and T. Erdogan, *Electron. Lett.*, 1993, **29**, 385.
5 M. G. Seats, G. R. Atkins and S. B. Poole, *Annu. Rev. Mater. Sci.*, 1993, **23**, 381.
6 T. E. Tsai, C. G. Askins and J. Friebele, *Appl. Phys. Lett.*, 1992, **61**, 390.
7 K. D. Simmons, S. La Rochelle, V. Mizrahi, G. I. Stegeman and D. L. Griscom, *Opt. Lett.*, 1991, **16**, 141.
8 L. Dong, J. L. Cruz, L. Reekie, M. G. Xu and D. N. Payne, *IEEE Photon. Technol. Lett.*, 1995, **7**, 1048.
9 K. D. Simmons, G. I. Stegeman, B. G. Potter Jr. and J. H. Simmons, *J. Non-Cryst. Solids*, 1994, **179**, 254.
10 L. Skuja, *J. Non-Cryst. Solids*, 1992, **149**, 77.
11 C. J. Brinker and G. W. Scherer, *Sol–Gel Science*, Academic Press Inc., San Diego, CA, 1990, ch. 3.
12 J. Livage, M. Henry and C. Sanchez, *Prog. Solid State Chem.*, 1988, **18**, 259.
13 C. Sanchez and J. Livage, *New J. Chem.*, 1990, **14**, 513.
14 R. C. Mehrotra, in *Sol–Gel Processing and Applications*, ed. Y. A. Attia, Plenum Press, New York, 1994, p. 41.
15 B. E. Yoldas, *J. Mater. Sci.*, 1979, **14**, 1843.
16 S. Acosta, P. Arnal, R. J. P. Corriu, D. Leclercq, P. H. Mutin and A. Vioux, *Mater. Res. Soc. Symp. Proc.*, 1994, **346**, 43.
17 T. A. Wark, E. A. Gulliver, L. C. Jones, M. J. Hampden-Smith, A. L. Rheingold and J. C. Huffman, *Mater. Res. Soc. Symp. Proc.*, 1990, **180**, 61.
18 C. Sanchez, J. Livage, M. Henry and F. Babonneau, *J. Non-Cryst. Solids*, 1988, **100**, 65.
19 M. J. Percy, J. R. Bartlett, J. L. Woolfrey, L. Spiccia and B. O. West, *J. Mater. Chem.*, 1999, **9**, 499.
20 L. G. Hubert-Pfalzgraf, S. Daniele, S. Boulmaaz and R. Papiernik, *Mater. Res. Soc. Symp. Proc.*, 1994, **346**, 21.
21 F. A. Cotton and G. Wilkinson, *Advanced Inorganic Chemistry*, J. Wiley and Sons, New York, 5th edn., 1988, p. 393.
22 N. Chiodini, F. Meinardi, F. Morazzoni, A. Paleari, R. Scotti and G. Spinolo, *Phys. Rev. B*, 1998, **58**, 9615.
23 M. J. Hampden-Smith, T. A. Wark, A. Rheingold and J. C. Huffman, *Can. J. Chem.*, 1991, **69**, 121.
24 J. Robertson, *J. Phys. C*, 1979, **12**, 4767.
25 L. Abello, B. Bochu, A. Gaskov, S. Koudryavtseva, G. Lucazeau and M. Roumyantseva, *J. Solid State Chem.*, 1998, **135**, 78.
26 M. Stapelbroek, D. L. Griscom, E. J. Friebele and G. H. Sigel Jr., *J. Non-Cryst. Solids*, 1979, **32**, 313.
27 D. L. Griscom, *Nucl. Instrum. Methods Phys. Res. B*, 1984, **1**, 481.
28 Y. Mizokawa and S. Nakamura, *Jpn. J. Appl. Phys.*, 1974, **2**, 253.
29 C. Canevali, N. Chiodini, P. Di Nola, F. Morazzoni, R. Scotti and C. L. Bianchi, *J. Mater. Chem.*, 1997, **7**, 997.
30 S. K. Sharma, J. F. Mammone and M. F. Nicol, *Nature*, 1981, **292**, 140.
31 F. L. Galeener, *Solid State Commun.*, 1982, **44**, 1037.
32 A. Pasquarello and R. Car, *Phys. Rev. B*, 1979, **20**, 3368.
33 F. L. Galeener, *Phys. Rev. B*, 1978, **19**, 4292.
34 R. A. Murray and W. Y. Ching, *Phys. Rev. B*, 1989, **39**, 1320.
35 E. Geissberger and F. L. Galeener, *Phys. Rev. B*, 1983, **28**, 3266.
36 N. Chiodini, F. Meinardi, F. Morazzoni, A. Paleari, R. Scotti and G. Spinolo, *Solid State Commun.*, 1998, **109**, 145.
37 R. S. Katiyar, P. Dawson, M. M. Hargreave and G. R. Wilkinson, *J. Phys. C, Solid State Phys.*, 1971, **4**, 2421.
38 J. Zuo, C. Xu, X. Liu, C. Wang, C. Wang, Y. Hu and Y. Qian, *J. Appl. Phys.*, 1994, **75**, 1835.
39 C. Xie, L. Zhang and C. Mo, *Phys. Status Solidi A*, 1994, **141**, K59.
40 K. N. Yu, Y. Xiong, Y. Liu and C. Xiong, *Phys. Rev. B*, 1997, **55**, 2666.

Paper 9/04415I